INL/CON-08-14276
PREPRINT

Design Configurations and Coupling High Temperature Gas-Cooled Reactor and Hydrogen Plant

TMCE 2008 Symposium

Chang H. Oh
Eung Soo Kim
Steven Sherman

April 2008

The INL is a
U.S. Department of Energy
National Laboratory
operated by
Battelle Energy Alliance

DESIGN CONFIGURATIONS AND COUPLING HIGH TEMPERATURE GAS-COOLED REACTOR AND HYDROGEN PLANT

Chang H. Oh
Thermal Fluids & Heat Transfer
Idaho National Laboratory
United States of America
Chang.Oh@inl.gov

Eung Soo Kim
Thermal Fluids & Heat Transfer
Idaho National Laboratory
United States of America
Eungsoo.Kim@inl.gov

Steven Sherman
Energy Security Department
Savannah River National Laboratory
United States of America
Steven.Sherman@srnl.doe.gov

ABSTRACT

The US Department of Energy is investigating the use of high-temperature nuclear reactors to produce hydrogen using either thermochemical cycles or high-temperature electrolysis. Although the hydrogen production processes are in an early stage of development, coupling either of these processes to the high-temperature reactor requires both efficient heat transfer and adequate separation of the facilities to assure that off-normal events in the production facility do not impact the nuclear power plant. An intermediate heat transport loop will be required to separate the operations and safety functions of the nuclear and hydrogen plants. A next generation high-temperature reactor could be envisioned as a single-purpose facility that produces hydrogen or a dual-purpose facility that produces hydrogen and electricity. Early plants, such as the proposed Next Generation Nuclear Plant (NGNP), may be dual-purpose facilities that demonstrate both hydrogen and efficient electrical generation. Later plants could be single-purpose facilities. At this stage of development, both single- and dual-purpose facilities need to be understood.

KEYWORDS

High temperature gas-cooled reactor, hydrogen plant, system integration, thermal hydraulics

1. INTRODUCTION

The Department of Energy is investigating the use of high-temperature nuclear reactors to produce hydrogen using either thermochemical cycles or high-temperature electrolysis. Although the hydrogen production processes are in an early stage of development, coupling either of these processes to the high-temperature reactor requires both efficient heat transfer and adequate separation of the facilities to assure that off-normal events in the production facility do not impact the nuclear power plant. An intermediate heat transport loop will be required to separate the operations and safety functions of the nuclear and hydrogen plants. Although an indirect electrical cycle would also require an intermediate loop similar to the loop required for hydrogen production, an electrical cycle would not be anticipated to have the same requirements for significant separation distances that hydrogen plant safety issues would require.

A next generation high-temperature reactor could be envisioned as a single-purpose facility that produces hydrogen or a dual-purpose facility that produces hydrogen and electricity. At the current time, it is anticipated that early plants may be dual-purpose facilities that demonstrate both hydrogen and efficient electrical generation, and that later plants could be single-purpose facilities. At this stage of development, both single- and dual-purpose facilities need to be understood.

Both helium and liquid salts are being considered as the working fluid in the intermediate heat transport loop. The liquid salts considered in this analysis included LiF-NaF-KF (Flinak) in molar concentrations of 46.5%, 11.5%, and 42%, respectively, and $NaBF_4$-NaF in molar concentrations of 92% and 8%. The use of a liquid salt provides the potential for improved heat transfer and reduced pumping powers, but also introduces materials compatibility issues.

This paper describes various intermediate heat transport loop configurations and summarizes the thermal-hydraulic, structural, and efficiency calculations that have been performed to characterize the advantages and issues associated with each configuration. The key issues that are addressed in this report include:

- Configuration options
- System parameters, such as temperature and pressure
- Working fluid options

A number of possible configurations for the high-temperature reactor primary coolant system and the intermediate heat transport loop have been identified. However, due to the page limit, only two configurations are presented in this paper. The ultimate objective of the program is to evaluate the advantages and disadvantages of each of the configurations and working fluids so that a specific design option can be recommended. However, the recommendation of a specific design requires input from a variety of disciplines related to materials, thermal-hydraulics, economics, safety, and plant operability. The purpose of this work is to evaluate the advantages and disadvantages of the configurations and working fluids to provide input to the decision making process.

2. DESIGN CONFIGURATIONS

A number of plant configurations were evaluated and results from two configurations are presented. For convenience, the following nomenclature is used relative to the heat exchangers:

- IHX - The first heat exchanger downstream of the NGNP outlet
- PHX - The heat exchanger that connects the intermediate heat transport loop to the hydrogen production plant
- SHX - The heat exchanger that, if present, is located between the IHX and the PHX, and is referred to as the secondary heat exchanger (SHX).

Figure 1 illustrates the indirect parallel system. The flow in the secondary coolant system is divided, with most of the flow going towards the PCU and the remainder going through a secondary heat exchanger (SHX) that directs heat towards the high temperature steam electrolysis (HTSE) plant. The flow through the hot side of the SHX is then mixed with the flow from the PCU to feed the cold side of the intermediate heat exchanger (IHX). However, some of the flow is diverted away from the PCU, which acts to decrease the efficiency of the cycle. There are three coolant loops. The primary coolant system contains the nuclear reactor, the hot side of the IHX, and a compressor. The secondary coolant system contains the cold side of the IHX, the hot side of the SHX, the PCU, and connecting piping, which is assumed to be short. The intermediate heat transport loop connects the secondary coolant system to the HTSE plant through several process heat exchangers (PHXs).

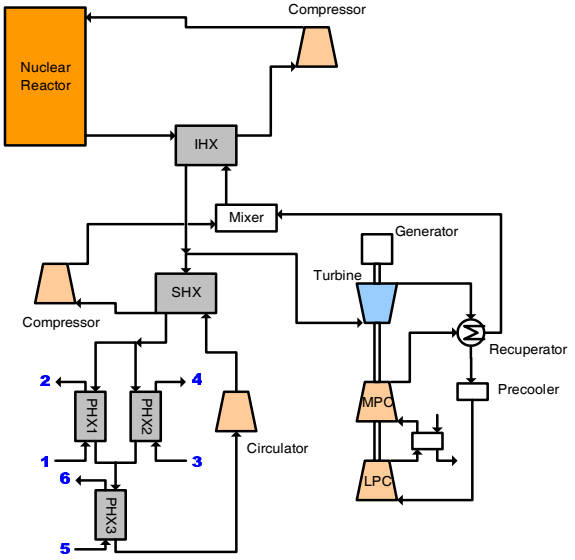

Figure 1 Configuration 1 - indirect parallel cycle

For electrolysis, the steam is heated up to higher than 800 °C by the heat from SHX. The heated steam is converted into hydrogen and oxygen in the electrolyzer and discharged through the fuel and oxidizer outlet, respectively as shown in Figure 2. The heat of the discharged gases is recovered through three recuperators. Finally, the product gas in the fuel side contains hydrogen and steam, and the oxidizer outlet gas contains oxygen and steam. As shown in Figure 2, the discharged fuel steam is recycled to the inlet fuel stream, and the hydrogen gas is separated and collected in the separator. In the oxidizer outlet stream

heat is first recuperated and then the stream is run through an expander to recover work. The oxygen and water components of the stream are then separated.

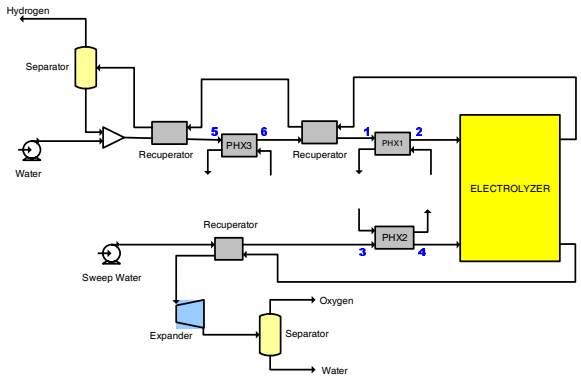

Figure 2 HTSE system

Figure 3 illustrates the indirect serial configuration. In this configuration, SHX is located upstream of the IHX that is linked to the PCU. Therefore, the heat from the VHTR is firstly transferred to the HTSE system, and then it is transferred to the PCU. This configuration is able to supply higher temperature to the HTSE system, but decreases the PCU maximum temperature, resulting in a decreased PCU efficiency. However, in this configuration, the system is more controllable due to its less connectivity. The reduction in the number of circulators can reduce the cost and increase the overall efficiency. The same HTSE system configuration as shown in Figure 2 is used here in terms of coupling the VHTR and the HTSE.

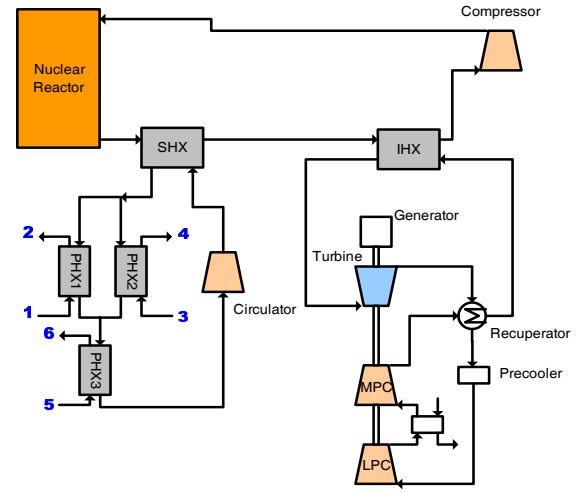

Figure 3 Configuration 2 - indirect serial cycle

Even though the indirect configuration was recommended by the Independent Technology Review Group [2004], the direct cycle was also considered in this study due to its simplicity, high efficiency, and economics. In this configuration, the primary side is integrated with the PCU, which leads to the elimination of the large IHX between the core and the PCU and the circulator in the primary side. As a result, it increases the efficiency and will reduce the capital cost. However, on the other hand, there will be some possibilities of safety and maintenance problems. In this configuration, the HTSE system is connected to VHTR through the SHX. The HTSE system is the same as the previous configurations. This paper includes only indirect cycle results.

3. METHODS

3.1. Component sizing

The nominal temperature drop between the outlet of the NGNP and the maximum temperature delivered to the hydrogen production plant is assumed to be 50 °C. This temperature drop imposes requirements on the effectiveness of the heat exchangers that connect the NGNP and the production plant and the amount of heat loss than can be tolerated in the intermediate loop. Although the total temperature drop between the NGNP and the production plant is fixed by assumption, the distribution of the temperature drop between the heat exchangers and heat loss can be varied. For example, if the heat loss can be reduced, the temperature drops across the heat exchangers can be increased and smaller heat exchangers can be used. After accounting for heat loss, the remaining temperature drop between the outlet of the NGNP and the maximum temperature delivered to the hydrogen production plant is divided evenly between the IHX, PHX, and, if present, the SHX.

As mentioned previously, the temperature drop between the NGNP and the production plant imposes requirements on the heat exchangers. The effectiveness of a heat exchanger, ε, (Kreith, 1964) can be calculated as

$$\varepsilon = \frac{(\dot{m}c_p)_h \, (T_{h\,in} - T_{h\,out})}{(\dot{m}c_p)_{min} \, (T_{h\,in} - T_{c\,in})} \tag{1}$$

where $\dot{m}$ is the mass flow rate, c_p is the specific heat capacity at constant pressure and is assumed constant, and T is the temperature. The subscripts h and c refer to the hot and cold sides of the heat exchanger, the subscripts in and out refer to the inlet and outlet ends of the heat exchanger, and the sub-

script min refers to the minimum value for the hot and cold sides.

The heat exchangers are assumed to be in counterflow, which requires less surface area than is required for parallel flow (Kreith, 1964). Counterflow heat exchangers are therefore smaller, and presumably cheaper, than corresponding heat exchangers in parallel flow. If the values of $\dot{m}c_p$ are the same for the hot and cold streams, the effectiveness depends only on the inlet and outlet temperatures.

Estimates are also made to size the heat exchangers. The required heat transfer area, A_{ht}, can be calculated from equations given by Kreith (1964)

$$A_{ht} = \frac{\varepsilon(\dot{m}c_p)_{min}\,(T_{h\,in} - T_{c\,in})}{U\,\Delta T} \tag{2}$$

where U is the overall heat transfer coefficient and ΔT is the log-mean temperature difference, which is calculated as

$$\Delta T = \frac{\Delta T_a - \Delta T_b}{\ln(\Delta T_a/\Delta T_b)} \tag{3}$$

where ΔT_a is the temperature difference between the hot and cold fluid streams at one end of the heat exchanger and ΔT_b is the temperature difference at the other end. The overall heat transfer coefficient is calculated from the heat transfer coefficients on both sides of the exchanger and the thermal conductivity and thickness of the metal. The heat transfer coefficients and the thermal conductivity are assumed constant over the length of the heat exchanger. For turbulent flow, the heat transfer coefficients are calculated using the Dittus-Boelter correlation, with a leading coefficient of 0.021 for gases and 0.023 for liquids (INEEL, 2003a). For laminar flow, the heat transfer coefficients are calculated from the exact solution for fully developed flow with constant heating rate (Kayes, Crawford 1980). The thermal conductivity of the metal is calculated assuming Alloy 800, and varies between 18 and 26 W/m-K over the temperature range of interest.

The pressure drop across a component is calculated from either the Blausius equation (Bird, et al., 1960) or the more accurate Zigrang-Sylvester correlation (INEEL, 2003b) for turbulent flow and the exact solution for fully developed laminar flow in a tube (Bird, et al., 1960).

3.2. Efficiency evaluation

The efficiency of each proposed configuration was estimated using HYSYS (Aspen Technology, 2005), a process optimization code used in the chemical and oil industries. Input models were developed for each of the configurations illustrated in Figures 1 and 2. The PCU cycle efficiency (Oh, 2005), η_{PCU}, used in this study is defined as:

$$\eta_{PCU} = \frac{\text{Electric power output}}{\text{Reactor thermal power} - \text{H}_2\text{ process power}} = \frac{\Sigma W_T - \Sigma W_C - W_S - \Sigma W_{CIR}}{Q_{th} - Q_{H2}} \tag{4}$$

where ΣW_T is the total turbine workload, ΣW_C is the total compressor workload, W_S is the plant stationary load, ΣW_{CIR} is the circulator workload in the primary, intermediate, and, if present, tertiary loops, Q_{th} is the reactor thermal power, and Q_{H2} is the power supplied through the PHX to the hydrogen generating plant. For the efficiency calculations, we report the overall cycle efficiency, which is defined as

$$\eta_{overall} = \frac{\Sigma W_T - \Sigma W_C - W_S - \Sigma W_{CIR} - \Sigma Q_{HTSE} + Q'_{H2}}{Q_{th}} \tag{5}$$

where ΣQ_{HTSE} is the electric power requirement for electrolysis and Q'_{H2} is the hydrogen production mass flow rate times the specific energy content of the hydrogen.

The polytropic efficiency, rather than the isentropic efficiency, is used for representing the efficiency of the turbomachinery. The equations for the expansion and compression processes in a perfect gas are taken from Saravanamuttoo et al. (1996). For an expansion, the efficiency is calculated from

$$\frac{T_{0,\,ex}}{T_{0,\,in}} = \left(\frac{P_{0,\,ex}}{P_{0,\,in}}\right)^{\left(\frac{R}{C_P}\eta_{p,\,e}\right)} \tag{6}$$

where R is the gas constant, C_p is the specific heat, $\eta_{p,\,e}$ is the turbine polytropic efficiency, T_0 is the stagnation temperature, and P_0 is the stagnation pressure. Subscripts ex and in refer to exit gas and inlet gas, respectively. For a compression, the efficiency is calculated from

$$\frac{T_{0,\,ex}}{T_{0,\,in}} = \left(\frac{P_{0,\,ex}}{P_{0,\,in}}\right)^{\left(\frac{R}{C_P}\frac{1}{\eta_{p,\,c}}\right)} \tag{7}$$

HYSYS was used to develop an input model for each configuration and working fluid and to optimize the

cycle efficiency. HYSYS uses the Peng-Robinson (1976) equation of state to determine the properties of the working fluids. However, HYSYS does not have thermal properties for molten salts. Therefore, the physical and thermal properties of Flinak and $NaBF_4$-NaF were input as hypothetical components in tabular form.

The efficiencies of the turbine and compressors were assumed to be 92% and 90%, respectively. Figures 1 and 2 show a single shaft connecting one turbine and one compressor. However, two compressors, a high-pressure compressor (HPC) and a low-pressure compressor (LPC), were used for better cycle efficiency. The pressure ratio, which is defined as the outlet pressure from the HPC divided by the inlet pressure to the LPC, was varied to optimize the overall cycle efficiency. Each compressor was assumed to provide half of the overall pumping power. Cooling was applied between compressors to reduce the power consumed by the HPC. Cooler components were used to simulate the heat loss and differential pressure along the hot and cold legs of the intermediate heat transport loop.

3.3. Hydrogen production modelling

The hydrogen production considered in this study is water splitting by the electrolysis ($H_2O \rightarrow H_2 + O_2$). A research program is under way at the Idaho National Laboratory (INL) to assess the performance of solid-oxide cells operating in the steam electrolysis mode for hydrogen production over a temperature range of 800 to 900 °C. The research program includes both experimental and modeling activities.

In the electrolyzer model (Oh, et al., 2006), the oxygen stream produced at the anode is assumed to mix with a sweep gas stream that is introduced at the anode. The combined stream then exits the electrolyzer. The hydrogen stream produced at the cathode is assumed to mix with a feed stream that is introduced at the cathode. The feed stream is composed of water vapor to be electrolyzed, hydrogen gas for maintaining reducing environment, and possibly an inert gas, presently assumed to be nitrogen.

An energy balance on the electrolyzer gives

$$\sum_i \dot{n}_{P-i}\, H_{P-i}\,(T_P, P) = \qquad (8)$$
$$= \sum_i \dot{n}_{R-i}\, H_{R-i}(T_R, P) \;+\; Q \;+\; W$$

where

$\dot{n}$ = species mole flow rate
H = enthalpy per mole
Q = rate of heat transfer to the electrolyzer
W = rate of electrical work supplied to the electrolyzer
T = temperature
P = pressure

and where we have used subscripts R for reactants and P for products. Their mass flowrates are defined

$$m_{H_2O-o-cath}\, h_{H_2O}\,(T_o,P) + m_{H_2-o-cath}\, h_{H_2}(T_o,P) + m_{N_2-o-cath}\, h_{N_2}(T_o,P)$$
$$m_{O_2-o-anode}\, h_{O_2}(T_o,P) + m_{sweep-o-anode}\, h_{sweep}(T_o,P) =$$
$$m_{H_2O-i-cath}\, h_{H_2O}\,(T_i,P) + m_{H_2-i-cath}\, h_{H_2}(T_i,P) + m_{N_2-i-cath}\, h_{N_2}(T_i,P)$$
$$m_{O_2-i-anode}\, h_{O_2}(T_i,P) + m_{sweep-i-anode}\, h_{sweep}(T_i,P) \;+\; Q + W \qquad (9)$$

where

m = species mass flow rate (kg/s)
h = specific enthalpy (joules/kg)

and where subscripts i and o represent inlet and outlet, respectively.

The species mole flowrates entering and leaving the electrolyzer are related to the current density through the relationships

$$\begin{aligned}
\dot{n}_{H_2O-o-cath} &= \dot{n}_{H_2O-i-cath} - \frac{iA}{2F} \\
\dot{n}_{H_2-o-cath} &= \dot{n}_{H_2-i-cath} + \frac{iA}{2F} \\
\dot{n}_{O_2-o-anode} &= \dot{n}_{O_2-i-anode} + \frac{iA}{4F} \qquad (10) \\
\dot{n}_{sweep-o-anode} &= \dot{n}_{sweep-i-anode} \\
\dot{n}_{N_2-o-cath} &= \dot{n}_{N_2-i-cath}
\end{aligned}$$

where

i = current density (amps/m^2)
A = electrode surface area, (m^2) and
F = Faradays constant

The species mass flowrates and mole flowrates are related as follows: for an individual species

$$\dot{m}_{k-o} = A_k \dot{n}_{k-o} \quad \text{and} \quad \dot{m}_{k-i} = A_k \dot{n}_{k-i} \qquad (11)$$
$$k = H_2O,\ H_2,\ O_2 \text{ and } N_2$$

where A_k is the atomic weight of species k in kg per mole and subscript o is the outlet and i is the inlet.

The voltage drop across the electrolyzer is the sum of the electrode Nernst potential and the resistance of

the cell. In estimating the resistance, the activation and the concentration overpotentials are lumped in with the cell internal resistance. The cell voltage is then assumed given by

$$V_{Nernst} = \overline{V}_{Nernst} + i \cdot ASR \tag{12}$$

where

$\overline{V}_{Nernst}$ = Nernst potential

ASR = area-specific cell resistance (ohms-m^2)

The electrical work done in the cell is

$$W = V_{cell} \cdot i \cdot A \tag{13}$$

The active species giving rise to the Nernst potential satisfy the chemical balance equation

$$H_2O\ (g)\ \rightarrow\ H_2\ (g)\ +\ \frac{1}{2}\,O_2\ (g) \tag{14}$$

The change in Gibbs free energy for this reaction carried out at temperature T and pressure P is

$$\Delta G(T,P) = \Delta G_f(T,P) + RT \ln \left[\frac{f_{H_2}\ f_{O_2}^{\frac{1}{2}}}{f_{H_2O}} \right] \tag{15}$$

where f is the molar fraction of a species and $\Delta G_f(T,P)$ is the Gibbs free energy in forming the products at temperature T and pressure P minus the same for the reactants, that is,

$$\Delta G_f(T,P) = G_{f-H_2}(T,P) + 1/2\, G_{f-O_2}(T,P) - G_{f-H_2O}(T,P) \tag{16}$$

where $G_{f-i}(T,P)$ is the Gibbs free energy on a per mole basis of forming species i at conditions T and P. In turn $\Delta G_f(T,P)$ is written in terms of $\Delta G_f^0(T) = \Delta G_f(T, P_{STD})$ where P_{STD} = 0.101 MPa. Then setting the change in Gibbs free energy equal to the electrical work done the voltage developed by the cell is

$$V_{Nernst} = \frac{-1}{2F}\left[\Delta G_f^0(T) + RT \ln \left[\left(\frac{f_{H_2} f_{O_2}^{\frac{1}{2}}}{f_{H_2O}} \right) \left(\frac{P}{P_{STD}} \right)^{\frac{1}{2}} \right]\right] \tag{17}$$

where P_{STD} = 0.101 MPa and P is the cell pressure. Then the average value of V_{Nernst} was calculated suing the following equation

$$\overline{V}_{Nernst} = \frac{1}{2F(T_P - T_R)(y_{o,O2,A} - y_{i,O2,A})(y_{o,H2,C} - y_{i,H2,C})} \times \int_{T_R}^{T_P} \int_{y_{i,O2,A}}^{y_{o,O2,A}} \int_{y_{i,H2,C}}^{y_{o,H2,C}} \Delta G\,(T) - RT \ln \left(\frac{1 - y_{H2} - y_{N2}}{y_{H2} y_{O2}^{1/2}} \right) dy_{H2}\, dy_{O2}\, dT \tag{18}$$

The mole fractions at any point in the electrolyzer are related to the molar mass flowrates at that point through

$$\begin{aligned} f_{H_2O-cath} &= \frac{\dot{n}_{H_2O}}{\dot{n}_{H_2O} + \dot{n}_{H_2} + \dot{n}_{N_2}} \\ f_{H_2-cath} &= \frac{\dot{n}_{H_2}}{\dot{n}_{H_2O} + \dot{n}_{H_2} + \dot{n}_{N_2}} \\ f_{O_2-anode} &= \frac{\dot{n}_{O_2}}{\dot{n}_{sweep} + \dot{n}_{O_2}} \\ f_{sweep-anode} &= \frac{\dot{n}_{sweep}}{\dot{n}_{sweep} + \dot{n}_{O_2}} \end{aligned} \tag{19}$$

The current density and active cell area are then specified, yielding the total operating current. Care must be taken to insure that the specified inlet gas flow rates and total cell current are compatible. The minimum required inlet steam molar flow rate is the same as the steam consumption rate, given by:

$$\begin{aligned} \dot{N}_{i,H2O,min} &= \Delta \dot{N}_{H2O} = \frac{I}{2F} N_{cells} \\ &= \frac{i\, A_{cell}}{2F} N_{cells} = \Delta \dot{N}_{H2} \end{aligned} \tag{20}$$

4. RESULTS

4.1. Configuration 1 – Indirect parallel cycle

Table 1 summarizes the calculated system efficiencies for Configuration 1. In this table, the primary flow loop includes the reactor core and the hot side of the IHX while the secondary loop includes the PCU and the ternary loop contains the intermediate heat transport loop that connects the SHX and the HTSE system. As a primary working fluid, Helium and Flinak were evaluated, as a secondary fluid, Helium and S-CO_2, and as a ternary fluid, Helium, S-CO_2, and Flinak were evaluated. A total of twelve different combinations of working fluids were evaluated.

In this calculation, Flinak in the primary loop increased the overall efficiency by 1.4% on average compared to Helium. Essentially, liquid phase (Flinak) requires less circulation power than the high

Table 1 Optimized efficiencies for Configuration 1

Primary	Secondary	Tertiary	Efficiency (%)
He	He	He	44.12
He	He	CO_2	44.47
He	He	Flinak	46.13
He	CO_2	He	43.35
He	CO_2	CO_2	43.5
He	CO_2	Flinak	43.41
Flinak	He	He	45.25
Flinak	He	CO_2	45.5
Flinak	He	Flinak	47.24
Flinak	CO_2	He	44.83
Flinak	CO_2	CO_2	45.06
Fliank	CO_2	Flinak	45.39

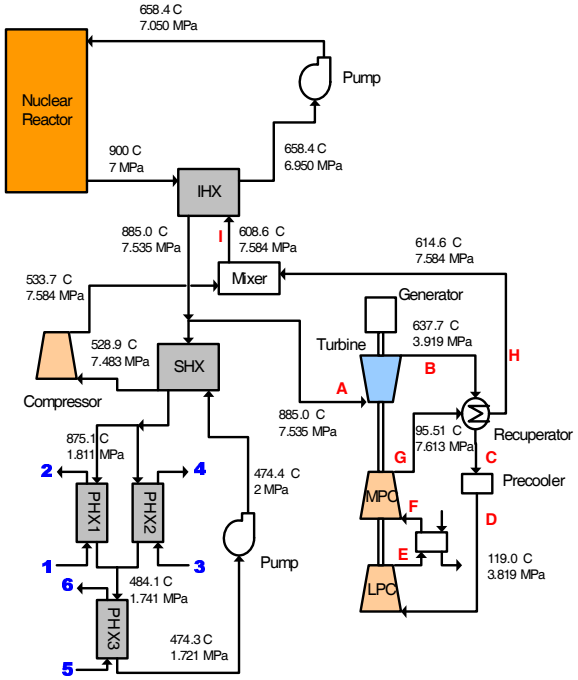

Figure 4 Plant operating conditions for Configuration 1 (Flinak–He–Flinak)

pressure gas phase (Helium). The highest efficiency using helium in the primary flow loop was achieved in Case 3 (He–He–Flinak) in Table 1 while Case 9 (Flinak–He–Flinak) resulted in the maximum overall efficiency. With this configuration, the flow rate of Flinak, 1318 kg/s, is three times higher than the one of He, 478.4 kg/s, however, its circulation power is only 1/140 of He (Flinak: 104.7 kW, He: 14770 kW). This results in a slight efficiency increase with

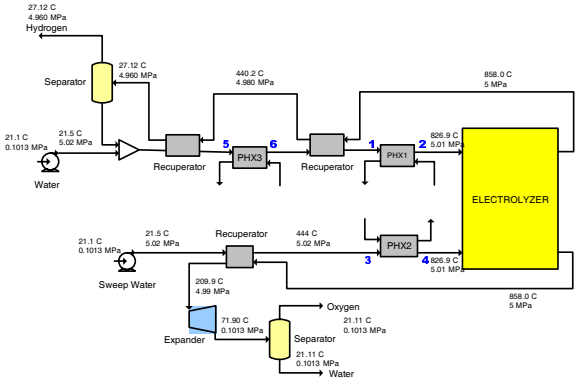

Figure 5 Operating conditions for the HTSE system

molten salt. Due to the higher density of the molten salt by a factor of 500 compared with that of Helium, we expect that Flinak system would require smaller core volume resulting in some economical advantages.

In the ternary loop, Flinak shows the highest performance due to the reduced pumping power compared with gas and as a result, approximately 0.5% of efficiency improvement was achieved on average. The reason why the improvement in the ternary loop is smaller than in the primary loop is that the circulation power of the ternary loop is much less than the primary loop.

From the above results, we could conclude that Flinak-He-Flinak system is the most effective working fluids in the primary, secondary and the ternary flow loop in terms of the overall system efficiency. The efficiency of this combination is 47.24%, the greatest of all combinations evaluated. Figures 4 and 5 illustrate the operating conditions for the optimized VHTR (Flinak–He–Flinak) and HTSE system, respectively. Figures 6 and 7 illustrate the P-V and T-S diagrams for the PCU in this system (Flinak–He–Flinak). These results will be benchmarked later with the HyPEP code.

4.2. Configuration 2 – Indirect serial cycle

The optimized results for the indirect serial cycle are summarized in Table 2. Like Configuration 1, the primary, secondary and ternary loops contain the reactor, the PCU, and the intermediate heat transport loop, respectively.

The maximum efficiency (48.38%) was obtained for Flinak-He-Flinak combination. It is due to the re-

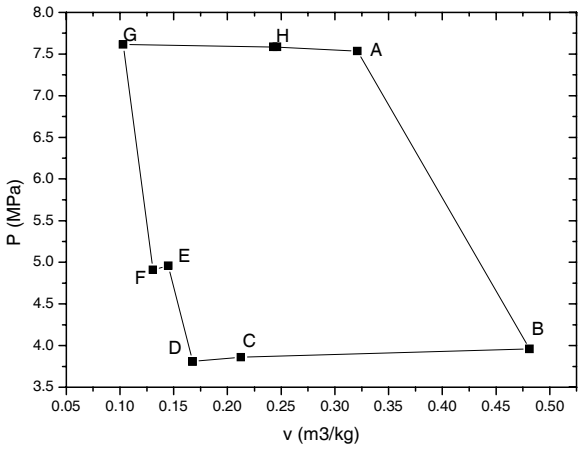

Figure 6 P-V diagram for Configuration 1 (Flinak–He–Flinak)

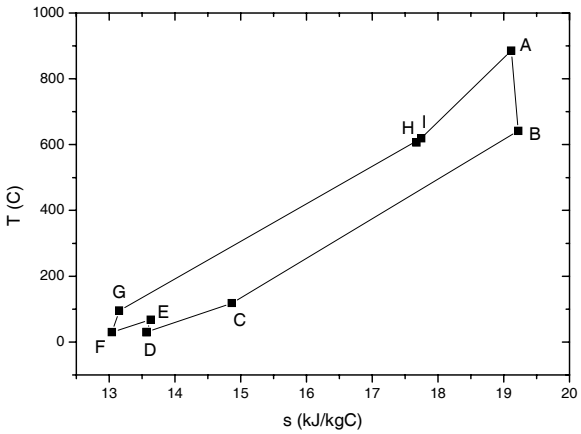

Figure 7 T-S diagram for Configuration 1 (Flinak–He–Flinak)

duction of circulation power for the primary and the ternary side caused by liquid coolant. As a result, the overall efficiency for Configuration 2 is about 1% higher than for Configuration 1, even though the turbine inlet temperature is a little reduced. The increase in efficiency is due to the decreased number of circulators. The elimination of one circulator and flow splitter is also expected to result in lower capital cost and higher controllability.

Figure 8 shows the optimized operating conditions for Configuration 2. Since the working fluid of the primary and the ternary loop is Flinak, the circulator in the original configuration (Figure 8) is changed to a pump. In the ternary loop, the minimum temperature is maintained above 454°C, the melting temperature of Flinak.

The core outlet temperature is maintained at 900°C,

Table 2 Optimized efficiencies for Configuration 2

Primary	Secondary	Tertiary	Efficiency (%)
He	He	He	46.26
He	He	CO_2	46.32
He	He	Flinak	46.32
He	CO_2	He	45.02
He	CO_2	CO_2	45.09
He	CO_2	Flinak	45.09
Flinak	He	He	48.13
Flinak	He	CO_2	48.3
Flinak	He	Flinak	48.38
Flinak	CO_2	He	46.9
Flinak	CO_2	CO_2	47.07
Fliank	CO_2	Flinak	47.15

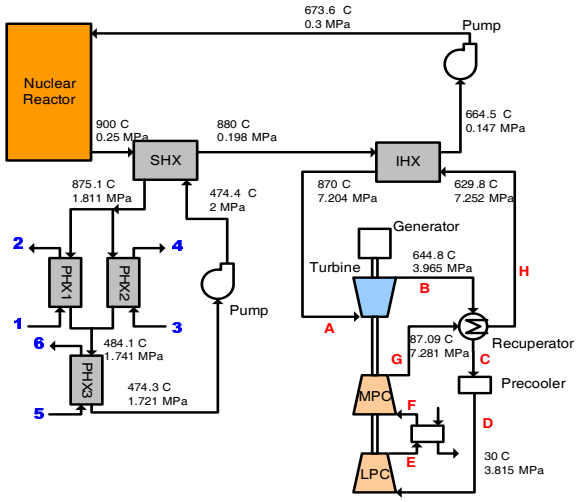

Figure 8 Optimized operating conditions for Configuration 2 (Flinak–He–Flinak)

and the optimal core inlet temperature is calculated to be 673.6°C by the energy balance around the VHTR. The effectiveness of the IHX and SHX was used as 0.95. The turbine inlet temperature (870°C) is little reduced compared with the Configuration 1 (885°C). At the optimal condition, the pressure ratio is 1.89. The operating conditions of the HTSE system are the same as for Configuration 1. Figures 9 and 10 illustrate the P-V and T-S diagrams for the optimized conditions (Flinak–He–Flinak).

5. CONCLUSIONS

A combined VHTR/HTSE system is one promising technology to produce hydrogen efficiently. In this study, the thermodynamic overall plant efficiency

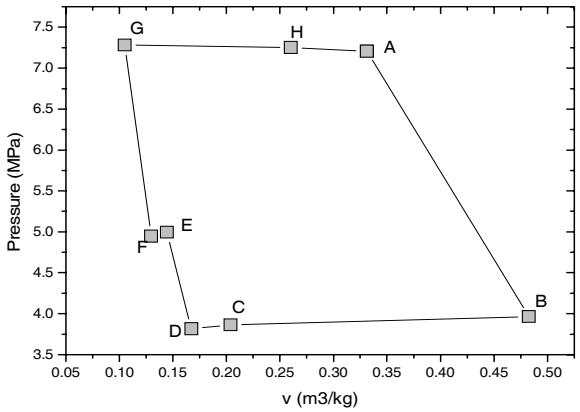

Figure 9 P-V diagram for Configuration 2 (Flinak–He–Flinak)

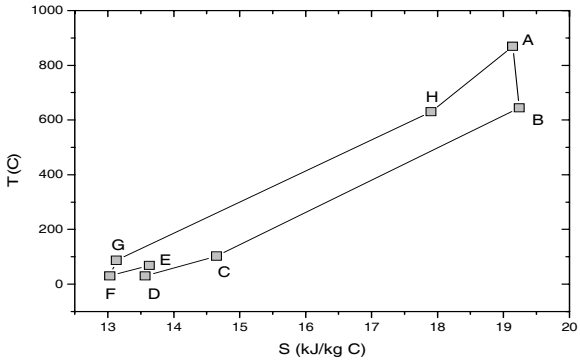

Figure 10 T-S diagram for Configuration 2 (Flinak–He–Flinak)

of the integrated system is evaluated using various configurations and working fluids. For these calculations, the reactor outlet temperature was fixed at 900 °C, which is the most sensitive factor for system efficiency.

The important result of this study is that we obtained very high efficiency even for the simple regeneration system. In case of indirect serial configuration, the optimal efficiency was 48.38% for Flinak-He-Flinak combination. In the serial system, since all the main components are independently separated, it may give much benefit for safety, maintenance and control problems. Although the parallel system resulted in a higher maximum temperature in the PCU, the maximum overall efficiency (47.24%) was a little lower than for the serial system because of the addition of one extra circulator.

The use of liquid Flinak almost always resulted in the highest efficiency for each configuration evaluated because the liquid phase coolant (Flinak) requires much less circulation power than the high pressure gas phase coolant. The relative benefit of Flinak was larger in the primary loop than in the ternary loop, with an average increase of about 1.5% in overall cycle efficiency for the primary loop versus about 0.6% for the ternary loop. The smaller benefit of Flinak in the ternary loop was due to the relatively smaller pumping power requirements compared to the primary loop. It is not clear if the increased efficiency in either loop is worth the capital cost associated with the facilities required for keeping the salt molten during shutdown and the materials issues associated with using molten salts at high temperatures.

The overall plant efficiency is also sensitive to the efficiencies of the compressor and turbine and the effectiveness of the heat exchanger, especially at low core inlet temperatures near 500 °C. Maintaining the performance of compressor, turbine and heat exchangers is essential for maintaining an efficient hydrogen production process.

ACKNOWLEDGMENT

This work was supported through the Department of Energy's ROK/US-INERI and Power Conversion Program under DOE Idaho Operations Office Contract DE-AC07-99ID13727.

REFERENCES

Bird, R. B., Stewart, W.E., Lightfoot, E. N., 1960, "Transport Phenomena", John Wiley & Sons, Inc., New York.

Dittus, F. W., Boelter, L. M. K., 1930, Univ. Calif. Berkeley Publ. Eng., vol. 2. pp. 433.

Independent Technology Review Group, 2004, "Design Features and Technology".

INEEL, 2003a, "RELAP5-3D Code Manual Volume 4: Models and Correlations", INEEL-98-00834, Revision 2.2.

INEEL, 2003b, "RELAP5-3D Code Manual Volume 1: Code Structure, System Models and Solution Methods", INEEL-98-00834, Revision 2.2.

Kayes, W. M., Crawford, M. E., 1980, "Convective Heat and Mass Transfer", Second Edition, McGraw-Hill Book Company, New York.

Kreith, F., 1964, "Principles of Heat Transfer", International Textbook Company, Scranton.

Oh, C., Moore, R., 2005, “Brayton Cycle for High Temperature Gas-Cooled Reactors”, Nuclear Technology, Vol. 149, pp. 324–336.

Oh, C. H., Kim, E. S., Sherman, S. R., Vilim, R., Lee, Y. J., Lee, W. J., 2007, “HyPEP FY-07 Annual Report: A Hydrogen Production Plant Efficiency Calculation Program”, INL/EXT-07-13078.

Peng, D. Y., Robinson, D. B., 1976, “A Two Constant Equation of State”, I.E.C. Fundamentals, 15, pp. 59–64.

Saravanamuttoo, H., et al., 1996, “Gas Turbine Theory”, Fifth Edition, Prentice Hall.